Experimental width shift distribution: a test of nonorthogonality for local and global perturbations

Jean-Baptiste Gros, Ulrich Kuhl, Olivier Legrand, Fabrice Mortessagne, Elodie Richalot, Dmitry Savin

Experimental width shift distribution: a test of nonorthogonality for local and global perturbations

J.-B. Gros,[1] U. Kuhl,[1,*] O. Legrand,[1] F. Mortessagne,[1] E. Richalot,[2] and D. V. Savin[3]

[1] *Université Nice Sophia Antipolis, CNRS, Laboratoire de Physique de la Matière Condensée, UMR 7336 Parc Valrose, 06100 Nice, France.*
[2] *Université Paris-Est, ESYCOM (EA 2552), UPEMLV, ESIEE-Paris, CNAM, 77454 Marne-la-Vallée, France*
[3] *Department of Mathematics, Brunel University, Uxbridge UB8 3PH, United Kingdom*

The change of resonance widths in an open system under a perturbation of its interior was recently introduced by Fyodorov and Savin [PRL **108**, 184101 (2012)] as a sensitive indicator of the nonorthogonality of resonance states. We experimentally study universal statistics of this quantity in weakly open two-dimensional microwave cavities and reverberation chambers realizing scalar and electromagnetic vector fields, respectively. We consider global as well as local perturbations, and also extend the theory to treat the latter case. The impact of the perturbation type on the width shift distribution is increasing with the number of open channels. We compare the theory to experimental results for one and two attached channels and to numerical simulations with higher channel numbers, observing a good agreement in all cases.

PACS numbers: 05.45.Mt, 03.65.Nk, 05.60.Gg

The most general feature of open quantum or wave systems is the set of complex resonances. They manifest themselves in scattering through sharp energy variations of the observables and correspond to the complex poles of the S matrix. Theoretically, the latter are given by the eigenvalues $\mathcal{E}_n = E_n - \frac{i}{2}\Gamma_n$ of the effective non-Hermitian Hamiltonian $\mathcal{H}_{\rm eff}$ of the open system [1–4]. The anti-Hermitian part of $\mathcal{H}_{\rm eff}$ originates from coupling between the internal (bound) and continuum states, giving rise to finite resonance widths $\Gamma_n > 0$. The other key feature is that the associated eigenfunctions become nonorthogonal [2, 4]. Their nonorthogonality is crucial in many applications; it influences nuclear cross-sections [5], features in decay laws of quantum chaotic systems [6], and yields excess quantum noise in open laser resonators [7]. For systems invariant under time reversal, like open microwave cavities studied below, the nonorthogonality is due to the complex wavefunctions, yielding the so-called phase rigidity [8–10] and mode complexness [11, 12]. Nonorthogonal mode patterns also appear in reverberant dissipative bodies [13], elastic plates [14], optical microstructures [15] and lossy random media [16].

Recently, an important connection was recognized in [17], identifying such nonorthogonality as the root cause for enhanced sensitivity of open systems to perturbations. Namely, one considers the parametric motion of complex resonances under a perturbation of the internal region. This can be modeled by a Hermitian term V added to $\mathcal{H}_{\rm eff}$, so $\mathcal{H}'_{\rm eff} = \mathcal{H}_{\rm eff} + V$. By applying perturbation theory for non-Hermitian operators [17, 18], the complex energy shift $\delta\mathcal{E}_n$ of the nth resonance in leading order reads

$$\delta\mathcal{E}_n \equiv \mathcal{E}'_n - \mathcal{E}_n = \langle L_n|V|R_n\rangle\,. \qquad (1)$$

$\langle L_n|$ and $|R_n\rangle$ stand for the left and right eigenfunctions of $\mathcal{H}_{\rm eff}$ indexed by the same (non-perturbed) eigenvalue $\mathcal{E}_n$. They form a biorthogonal system; in particular, $\langle L_n|R_m\rangle = \delta_{nm}$ but $U_{nm} \equiv \langle L_n|L_m\rangle \neq \delta_{nm}$ in general. U is known in nuclear physics as the Bell-Steinberger nonorthogonality matrix [2, 5], see also [19]. Crucially, a nonzero value of the width shift, $\delta\Gamma_n = -2{\rm Im}\,\delta\mathcal{E}_n$, is induced solely by the *off-diagonal* elements U_{nm}, as is clearly seen from the following representation [17]:

$$\delta\Gamma_n = i\sum_m (U_{nm}V_{mn} - V_{nm}U_{mn})\,, \qquad (2)$$

where $V_{nm} = \langle R_n|V|R_m\rangle = V^*_{mn}$. The width shift (2) is therefore an indicator of the nonorthogonality, vanishing only if the resonance states were orthogonal.

Note that the nonorthogonality measures studied in [7–12] are related to the *diagonal* elements U_{nn}. Those and the width shift (2) contain complementary information on nonorthogonality. In particular, the off-diagonal elements U_{nm} are parametrically stronger for weakly open systems, when the widths Γ are small compared to the level spacing Δ ($\Gamma \ll \Delta$): then $U_{n\neq m} \sim \frac{\Gamma}{\Delta}$ [17] whereas $U_{nn} - 1$ is only of the order of $\left(\frac{\Gamma}{\Delta}\right)^2$ [12]. Thus the width shift (2) is more sensitive to nonorthogonality effects.

In this Letter, we report the first experimental study of the width shift statistics for fully chaotic systems using microwave cavities of different kinds. We consider both local and global perturbations and also investigate whether a different behaviour occurs in the scalar case (two-dimensional billiards) and the vectorial case (reverberation chambers). Additionally, we perform numerical simulations for the latter case, where the system's openness is introduced by local absorption.

Global vs local perturbations.— Analytical treatment of chaotic systems usually deals with statistical modeling based on random matrix theory [20, 21]. We consider below only weakly open systems with time-reversal

symmetry. The energy levels are then induced by the eigenvalues of a random matrix drawn from the Gaussian orthogonal ensemble (GOE). Those N levels are coupled through the anti-Hermitian part of $\mathcal{H}_{\rm eff}$ to M open channels [1, 2], which are assumed to be statistically equivalent and characterized by the coupling strength κ. In the regime of weak coupling, $\kappa \ll 1$, the resonance positions E_n are given just by those eigenvalues, revealing universal fluctuations on the local scale of $\Delta \sim \frac{1}{N}$ in the limit $N \gg 1$. Correspondingly, the wave function components become Gaussian distributed random variables, yielding the well-known χ^2_M distribution for the resonance widths,

$$P_M(\gamma) = \frac{1}{2^{M/2}\Gamma(M/2)} \gamma^{M/2-1} e^{-\gamma/2} \,. \qquad (3)$$

Here, we have expressed the widths $\gamma_n = \Gamma_n/\overline{\Gamma}$ in units of the average partial width $\overline{\Gamma} = 2\kappa\Delta/\pi$. With the variance $\mathrm{var}(\gamma) = \frac{2}{M}\langle\gamma\rangle$, distribution (3) becomes sharply peaked around its mean $\langle\gamma\rangle = M$ when $M \gg 1$ [2, 3].

To describe both local and global perturbations on equal footing, we follow [22, 23] and represent the perturbation term as $V = \sum_{q=1}^{r} \alpha_q |q\rangle\langle q|$. Its rank r governs the transition between the local (r small) and global ($r \gg 1$) case. One can interpret V as r point scatterers characterized by the strength coefficients α_q. For example, a single scatterer added to the system induces an energy shift $\delta E_n = \langle n|V|n\rangle = \alpha\psi_n^2(q)$ for the nth level, with $\psi_n(q) = \langle q|n\rangle$ being the wave function component at point q. However, moving the scatterer from point q to q', what we did in our experiment (see Fig. 1), results in the shift $\delta E_n = \alpha(\psi_n(q)^2 - \psi_n(q')^2)$. The latter is equivalent to a rank-2 perturbation with $V = \alpha(|q\rangle\langle q| - |q'\rangle\langle q'|)$ [23]. Generally, the variance of the energy shifts is given by $\mathrm{var}(\delta E_n) = \frac{2}{N^2}\mathrm{tr}(V^2)$, which sets up a scale for the parametric level dynamics [24]. Importantly, the rescaled energy shifts $\sim \delta E_n/\sqrt{\mathrm{var}(\delta E_n)}$ (also called 'level velocities') acquire universal fluctuations of a distinct type in the case of local and global perturbations, being given by a K_0 distribution (for $r = 2$) [25] and Gaussian, respectively. A gradual transition between the two occurs quickly as the perturbation rank r grows [23].

For the width shifts at $\kappa \ll 1$, it was shown in [17] that the assumption of the Gaussian distributed wave functions results in the following representation for the rescaled width shifts ('width velocities'):

$$y_n \equiv \frac{\delta\Gamma_n}{2\kappa\sqrt{2\mathrm{var}(\delta E_n)}} = \frac{\sqrt{\gamma_n}}{\pi} \sum_{m\neq n} \frac{z_m v_m \Delta}{E_n - E_m} \,. \qquad (4)$$

Here, real z_m are normally distributed random variables (stemming from coupling to the channels) whereas real $v_m = N\langle m|V|v\rangle/\sqrt{\mathrm{Tr}(V^2)}$ are the normalized matrix elements ($m\neq n$) of the perturbation. These quantities are statistically independent, which is a result of separating independent fluctuations in spectra and in wave functions of weakly open chaotic systems.

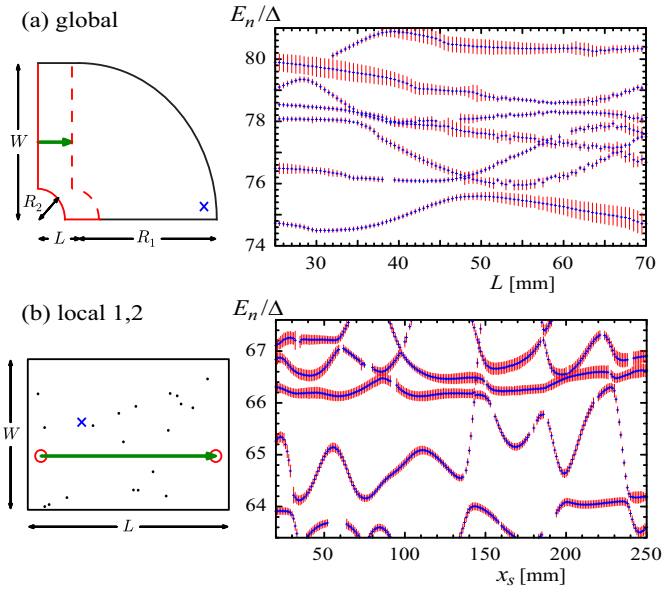

FIG. 1. (color online). The experimental setup (left) together with the parametric dependence (right) of the Weyl normalized energies (+) and widths (red vertical lines) for two microwave cavities: (a) Sinai stadium with a movable wall (R_1=W=240 mm, R_2=50 mm), L ranging from 1.5 to 70.5 mm in steps of 0.5 mm. (b) Rectangular billiard (L=340 mm, W=240 mm) with 19 randomly placed scatterers (black dots) of radius r_c=2.3 mm. One additional scatterer (red open circle) with radius r_{p1}=2.3 mm or r_{p2}=9.75 mm was moved along the green arrow in steps of δr=1 mm or 0.5 mm, respectively, from the starting position (x_s,y_s)=(20,85) mm to the final one (x_s,y_s)=(320,85) mm (the origin is at the lower left corner). The blue crosses mark the antenna position. The parameter axis is the change of the billiard length L in (a), and the scatterer position along the line x_s in (b).

To characterize universal statistics of the width velocities (4), we compute their probability distribution function, $\mathcal{P}_M(y) = \Delta\langle\sum_{n=1}^{N}\delta(E_n)\delta(y-y_n)\rangle$. Making use of the convolution theorem, it can be cast as follows [17]

$$\mathcal{P}_M(y) = \int_0^\infty \frac{d\gamma}{\sqrt{\gamma}} P_M(\gamma)\, \phi\left(\frac{y}{\sqrt{\gamma}}\right) , \qquad (5)$$

where the function $\phi(y)$ is defined by

$$\phi(y) = \int_{-\infty}^{\infty} \frac{d\omega}{2\pi} e^{i\omega y} \left\langle \prod_{m\neq n} \exp\left\{-i\frac{\omega z_m v_m}{\pi E_m/\Delta}\right\}\right\rangle . \qquad (6)$$

For global perturbations, the quantities v_m become normally distributed random variables [17], which makes the averaging over $\{z_m, v_m\}$ straightforward. The resulting expression can be then reduced to the GOE average of certain spectral determinants, which was also derived in [17], with the explicit form of ϕ being

$$\phi^{(\rm gl)}(y) = \frac{4+y^2}{6(1+y^2)^{5/2}} \,. \qquad (7)$$

When substituted into (5), it leads to the distribution of the width velocities in this (global) case, $\mathcal{P}_M^{(\mathrm{gl})}(y)$.

The case of local perturbations is more tricky, due to less trivial statistics of v_m. However, an exact result can be found in the particular case of r equivalent scatterers (all $|\alpha_p| = \alpha$), which is of interest here. To this end, we first treat $v_m = \frac{N}{\sqrt{r}}(\psi_m \cdot \psi_n)$ as a scalar product of two r-dimensional vectors of the wave function components and parametrize it as $v_m = \frac{\sqrt{\eta_n}}{\sqrt{r}}\nu_m$ in terms of their magnitudes $\sqrt{\eta_n}$ and the projection ν_m. The advantage of such a parametrization is that ν and η are statistically independent [12], with a normal and χ_r^2 distribution [cf. Eq. (3)], respectively. Then one can readily perform a Gaussian integration over $\{z_m, \nu_m\}$ in (6), arriving at

$$\phi_r^{(\mathrm{loc})}(y) = \left\langle \frac{\sqrt{r}}{\sqrt{\eta}} \phi^{(\mathrm{gl})}\left(\frac{\sqrt{r}y}{\sqrt{\eta}}\right)\right\rangle_\eta , \qquad (8)$$

where $\phi^{(\mathrm{gl})}$ is given by Eq. (7) and the remaining average over η is left at the end [26]. Combination of Eqs. (5) and (8) solves the problem exactly at arbitrary rank r.

Functional dependencies of $\phi_r^{(\mathrm{loc})}(y)$ and $\phi^{(\mathrm{gl})}(y)$ are the same in the tails and differ only in the bulk, but their difference diminishes quickly as r grows. For small channel numbers, the difference becomes even less noticeable for the width velocity distribution $\mathcal{P}_M(y)$, e.g. see Fig. 2, due to the additional integration in Eq. (5) over the widths. Since the width distribution (3) tends to $\delta(\gamma - M)$ as $M \to \infty$, one has $\mathcal{P}_{M\gg 1}(y) = \frac{1}{\sqrt{M}}\phi_r^{(\mathrm{loc})}(\frac{y}{\sqrt{M}})$ as the limiting distribution of the width velocities in this case. Hence, many-channel systems turn out to be more sensitive to the impact of finite r than their few channel analogues. We also mention the general power-law decay $\mathcal{P}_M(y) \propto |y|^{-3}$ of the distribution at $|y| \gg 1$, which can be linked to the linear level repulsion [17]. Such tails get exponentially suppressed in chaotic systems with rigid spectra without spectral fluctuations [12, 27].

Scalar experiments.— To investigate the statistics of the width velocity for scalar fields we use cylindrical (two-dimensional) microwave cavities, where the z-component of the electric field corresponds to the quantum wave function ψ and the wavenumber k^2 to the energy E [28]. Their heights are 8 mm leading to a cutoff frequency of $\nu_{\mathrm{cut}} = 18.75\,\mathrm{GHz}$. Figure 1 shows the three different systems. The first one is a chaotic Sinai-stadium billiard [see Fig. 1(a)] which we will denote as global perturbation. We used the range from the 50th to 100th resonance for the width velocity distribution. The second (third) system is a rectangular cavity with 19 scatterers, where an additional scatterer with the same (a larger) radius was moved [for further details see Fig. 1(b)], being denoted by local 1 (local 2). Again we took resonances from the 50th to 100th (85th) for the local 1 (2) case. All three systems are chaotic and in the ballistic regime.

As the resonances for the three systems are well isolated in this frequency regime, the complex eigenfrequencies have been obtained by Lorentzian fitting. In all cases we normalize the energies and widths to the mean level spacing Δ by using the Weyl formula given by $E_n/\Delta = \pi A(\nu_n/c)^2 + P(\nu_n/c)$, where ν_n, A and P are the eigenfrequency, area and circumference, respectively. In case of the global perturbation, this unfolding also removes the global energy shift due to the area change.

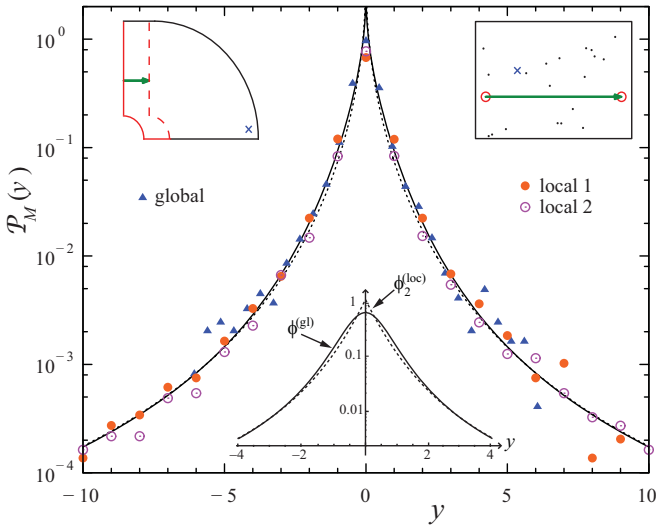

FIG. 2. (color online). Distribution of the experimental normalized width velocities y for three systems corresponding to Fig. 1: Sinai-stadium (global, ▲), rectangular billiard with scatterers and one small (local 1, ●) or larger (local 2, ⊙) movable perturber. The solid (dashed) curve stand for the theoretical prediction for the global (local, r=2) perturbation at $M = 1$, according to Eqs. (5), (7) and (8). The lower inset shows the corresponding behavior of function (8).

In Fig. 1, we also show the dependence of the complex eigenvalues on the parameter for the global and local level dynamics. The blue crosses indicate the resonance positions in the units of Δ, whereas the length of the red vertical lines corresponds to the width. A distinct difference in the parametric dynamics of the level velocities (i.e. the change of E_n with the perturbation) for the global and local perturbations is already visible here. The level velocity distribution is Gaussian in the global case, whereas it is a K_0 distribution in the local case, both cases have been experimentally studied in [25, 29]. Notably, such differences are much less pronounced for the width velocities, as already discussed before.

In the theoretical description of the width velocities (4) only two parameters enter: the antenna coupling and the variance of the level velocities. Both can be fixed in advance. The antenna coupling can be calculated by [30]

$$\kappa = \frac{|1 - \langle S_{11}\rangle_{\nu,p}|^2}{1 - |\langle S_{11}\rangle_{\nu,p}|^2}, \qquad (9)$$

where special care has been taken to remove global phase shifts induced by the antennas. The average has been

performed over the whole investigated frequency range and for all parameters. We find $\kappa_1 = 0.180$ (global), $\kappa_2 = 0.065$ (local 1) and $\kappa_3 = 0.098$ (local 2). In principle, one has to incorporate also the width $\Gamma_{w,n}$ induced by the additional absorption due to the finite conductance within the metallic walls. These effects have to be taken into account if one looks into the width distribution [31]. Here, we assume that $\Gamma_{w,n}$ as a function of the parameter stays constant or induces much smaller variations than the change induced by the coupled antenna and therefore can be neglected for the width velocity distribution. Note that we do not assume that $\Gamma_{w,n}$ is the same for all resonances [11, 32, 33].

Now we look at the experimental distributions of the normalized width shifts y_n, which are presented in Fig. 2. The normalization of the width Γ_n takes into account the variance of the real parts and the coupling extracted as mentioned before. As M is fixed by the number of attached antennas, i.e. $M = 1$, there is no free parameter in the comparison of the experimental results and the theory. In all cases, we find good agreement with the corresponding theoretical predictions. However, the amount of statistics is not sufficient to distinguish between the global and local perturbations in the width velocity distribution. At the only point where this would be possible from the statistical point of view (y close to 0), the experimental approximation of neglecting effects induced by absorption becomes not valid any more. To this end, we have seen that the width shift is a good quantity to indicate the nonorthogonality of the eigenfunctions, difficult to be extracted by other means.

Vectorial electromagnetic cavities.— To support the validity of this test of nonorthogonality in the three dimensional case for electromagnetic vector fields, we now present experimental results as well as numerical simulations in a chaotic reverberation chamber (RC). We also emphasize the dependence on the number of channels M through various types of losses induced in the cavity either through an antenna or locally distributed Ohmic dissipation at walls. The experiments were performed in a commercial reverberation chamber that was made chaotic by adding three metallic half-spheres on the walls, see the inset on Fig. 3. The parametric variation is ensured by an asymmetric stirrer which can be rotated around a vertical axis. The chaotic character of this cavity has been checked through the methodology described in Ref. [34]. The volume of the RC is approximately $V = 19\,\mathrm{m}^3$ and measurements were performed via either one single dipole antenna connected in a wall or between the latter antenna and a monopole antenna placed inside the cavity far from all the walls. These two situations correspond to $M = 1$ and $M = 2$ coupling channels, respectively. The measurements were performed at 10^4 excitation frequencies regularly spaced in a band of 20 MHz centered around 400 MHz (corresponding to the 372th resonance of the RC), for 128 ($M = 1$) or 90 ($M = 2$)

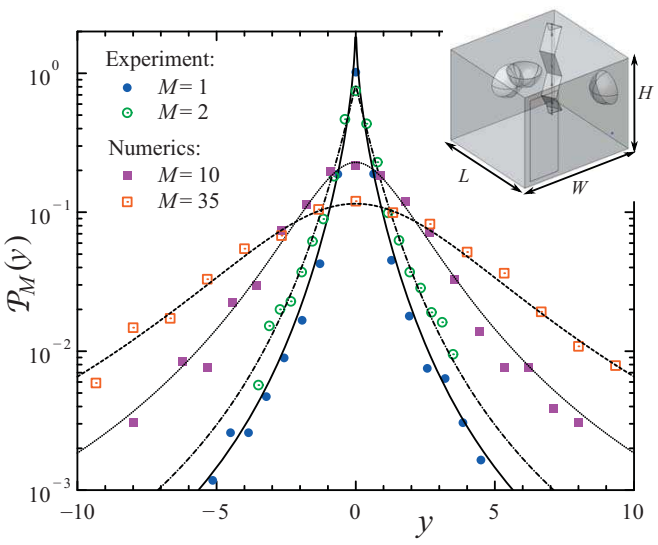

FIG. 3. (color online). Distribution of the width velocities for several configurations of the chaotic reverberation chamber with rotating stirrer (shown in the inset). Experimental realization with M=1 (•) and M=2 (⊙) and two numerical configurations presented in the main text with M=10 (■) and M=35 (⊡). The lines stand for the corresponding analytical results. For the normalization of the width shifts a fitted value of the coupling was used, yielding $\kappa_{M=1} = 0.45$, $\kappa_{M=2} = 0.16$, $\kappa_{M=10} = 0.049$, and $\kappa_{M=35} = 0.019$.

positions of the rotating stirrer (acting as a global perturbation) spaced by 1 degree. The mean quality factor is about 2500, corresponding to a moderate average modal overlap of $d = \langle\Gamma\rangle/\Delta \simeq 0.4-0.5$. Here we extract around 70 resonance frequencies and their widths for each position of the rotating stirrer by means of the harmonic inversion [31]. The resulting distributions of widths are shown in Fig. 3 (full and empty circles). In these specific cases, we have used again that the dominant contribution to the parametric fluctuations of widths comes from the coupling antenna(s), whereas the other types of losses (Ohmic dissipation at walls, junction defects, etc.) have negligible effects. This is further supported by the fair agreement with the analytical predictions for global perturbation at M=1, 2, as illustrated on Fig. 3 [35]. Thus the width shift distribution, theoretically obtained for quantum chaotic systems, i.e. scalar fields, appears to be valid also for vectorial electromagnetic fields.

It is difficult to investigate the role of higher number of channels experimentally since the coupling of each antenna would have to be reduced, leading to too small signal to noise ratios for any practical extraction of the complex resonances. Moreover, in such a case, all the type of losses would become of the same order as those induced by antennas. Therefore, we performed numerical calculations using a finite-element method and calculated the resonances of two different configurations of the chaotic RC described in [34, 36], where the coupling was

mimicked by local absorption at the boundaries through ohmic dissipative square patches scattered over the walls. All the patches have the same size, and both their conductivity and their number can be adjusted in order to obtain a specific value of the quality factor and to control the effective number of equivalent weakly coupling channels. Since then the width distribution is given by eq. (3), one can deduce the effective number of channels from $M/2 = \langle\Gamma\rangle^2/\mathrm{var}(\Gamma)$, which is also found to be valid for reasonably moderate modal overlap [32, 37]. The coupling strength can be estimated by

$$\kappa \simeq \pi d/(2M)\,. \tag{10}$$

For the two configurations investigated, we obtained $M = 10$, $d = 0.34$, and $\kappa_{10} = 0.05$ in one case and $M = 35$, d=0.51, and $\kappa_{35} = 0.024$ in the other. For both configurations, the width velocity distributions are shown on Fig. 3 (full and empty squares) where the fitted values of κ are $\kappa_{M=10} = 0.049$ and $\kappa_{M=35} = 0.019$, respectively, which are very close to the expected values. Again, we find an excellent agreement with the theoretical predictions, extending our findings for the experimental results.

In conclusion, we experimentally verified the theoretical results for the width shift distribution [17] for global perturbations for scalar as well as for electromagnetic vectorial fields, supporting universal statistics of width shift fluctuations in weakly open wave chaotic systems. Additionally, we extended the theoretical approach to arbitrary rank perturbation which was also found to be in good agreement with our experimental findings.

We acknowledge support by the ANR via the project CAOREV.

* Corresponding author, email: ulrich.kuhl@unice.fr

[1] J. J. M. Verbaarschot, H. A. Weidenmüller, and M. R. Zirnbauer, Phys. Rep. **129**, 367 (1985).
[2] V. V. Sokolov and V. G. Zelevinsky, Nucl. Phys. A **504**, 562 (1989).
[3] Y. V. Fyodorov and H.-J. Sommers, J. Math. Phys. **38**, 1918 (1997).
[4] I. Rotter, J. Phys. A: Math. Theor. **42**, 153001 (2009).
[5] V. V. Sokolov, I. Rotter, D. V. Savin, and M. Müller, Phys. Rev. C **56**, 1044 (1997).
[6] D. V. Savin and V. V. Sokolov, Phys. Rev. E **56**, R4911 (1997).
[7] H. Schomerus, K. M. Frahm, M. Patra, and C. W. J. Beenakker, Physica A **278**, 469 (2000).
[8] P. W. Brouwer, Phys. Rev. E **68**, 046205 (2003).
[9] Y.-H. Kim, U. Kuhl, H.-J. Stöckmann, and P. W. Brouwer, Phys. Rev. Lett. **94**, 036804 (2005).
[10] E. N. Bulgakov, I. Rotter, and A. F. Sadreev, Phys. Rev. E **74**, 056204 (2006).
[11] D. V. Savin, O. Legrand, and F. Mortessagne, Europhys. Lett. **76**, 774 (2006).
[12] C. Poli, D. V. Savin, O. Legrand, and F. Mortessagne, Phys. Rev. E **80**, 046203 (2009).
[13] O. I. Lobkis and R. L. Weaver, J. Acoust. Soc. Am. **108**, 1480 (2000).
[14] O. Xeridat, C. Poli, O. Legrand, F. Mortessagne, and P. Sebbah, Phys. Rev. E **80**, 035201(R) (2009).
[15] J. Wiersig, S. W. Kim, and M. Hentschel, Phys. Rev. A **78**, 053809 (2008); J. Wiersig, Phys. Rev. A **84**, 063828 (2011).
[16] N. Bachelard, C. Garay, J. Arlandis, R. Touzani, and P. Sebbah (2014), preprint arXiv:1407.8220.
[17] Y. V. Fyodorov and D. V. Savin, Phys. Rev. Lett. **108**, 184101 (2012).
[18] T. Kato, *Perturbation Theory for Linear Operators* (Springer-Verlag, New York, 1966).
[19] J. T. Chalker and B. Mehlig, Phys. Rev. Lett. **81**, 3367 (1998).
[20] T. Guhr, A. Müller-Groeling, and H. A. Weidenmüller, Phys. Rep. **299**, 189 (1998).
[21] Y. V. Fyodorov and D. V. Savin, in *Oxford Handbook of Random Matrix Theory*, edited by G. Akemann, J. Baik, and P. Di Francesco (Oxford University Press, UK, 2011), pp. 703–722; arXiv:1003.0702.
[22] I. L. Aleiner and K. A. Matveev, Phys. Rev. Lett. **80**, 814 (1998).
[23] F. M. Marchetti, I. E. Smolyarenko, and B. D. Simons, Phys. Rev. E **68**, 036217 (2003).
[24] Y. V. Fyodorov and A. D. Mirlin, Phys. Rev. B **51**, 13403 (1995).
[25] M. Barth, U. Kuhl, and H.-J. Stöckmann, Phys. Rev. Lett. **82**, 2026 (1999).
[26] For example, one finds $\phi_2^{(\mathrm{loc})}(y) = \frac{1}{3}[\sqrt{\pi}e^{y^2}\mathrm{erfc}(|y|)(2y^4+7y^2+2) - 2|y|(y^2+3)]$ at r=2 (one movable scatterer).
[27] D. V. Savin and J.-B. De Vaulx, Acta Phys. Pol. A **124**, 1074 (2013).
[28] H.-J. Stöckmann and J. Stein, Phys. Rev. Lett. **64**, 2215 (1990); J. Stein and H.-J. Stöckmann, Phys. Rev. Lett. **68**, 2867 (1992).
[29] M. Barth, U. Kuhl, and H.-J. Stöckmann, Ann. Phys. (Leipzig) **8**, 733 (1999).
[30] B. Köber, U. Kuhl, H.-J. Stöckmann, T. Gorin, D. V. Savin, and T. H. Seligman, Phys. Rev. E **82**, 036207 (2010).
[31] U. Kuhl, R. Höhmann, J. Main, and H.-J. Stöckmann, Phys. Rev. Lett. **100**, 254101 (2008).
[32] C. Poli, O. Legrand, and F. Mortessagne, Phys. Rev. E **82**, 055201(R) (2010).
[33] U. Kuhl, O. Legrand, and F. Mortessagne, Fortschritte der Physik **61**, 404 (2013).
[34] J.-B. Gros, O. Legrand, F. Mortessagne, E. Richalot, and K. Selemani, Wave Motion **51**, 664 (2014).
[35] We note that we fitted κ using the distribution as we were not able to extract its value by Eq. (9), due to a frequency dependent phase induced by the antennas.
[36] J.-B. Gros, U. Kuhl, O. Legrand, F. Mortessagne, O. Picon, and E. Richalot, to be published (2014).
[37] J.-B. Gros, U. Kuhl, O. Legrand, and F. Mortessagne, in preparation (2014).